Spatiotemporal Organization of Touch Information in Tactile Neuron Population Responses

Neeli Tummala
Electrical and Computer Engineering
University of California, Santa Barbara
Santa Barbara, USA
ntummala@ucsb.edu

Yitian Shao
Electrical and Computer Engineering
CeTI, Technische Universität Dresden
Dresden, Germany
yitian.shao@tu-dresden.de

Yon Visell
College of Engineering
University of California, Santa Barbara
Santa Barbara, USA
yonvisell@ucsb.edu

***Abstract*—Manual touch interactions elicit widespread skin vibrations that excite spiking responses in tactile neurons distributed throughout the hand. The spatiotemporal structure of these population responses is not yet fully understood. Here, we evaluate how touch information is encoded in the spatiotemporal organization of simulated Pacinian corpuscle neuron (PC) population responses when driven by a vibrometry dataset of whole-hand skin motion during commonly performed gestures. We assess the amount of information preserved in these peripheral population responses at various spatiotemporal scales using several non-parametric classification methods. We find that retaining the spatial structure of the whole-hand population responses is important for encoding touch gestures while conserving the temporal structure becomes more consequential for gesture representation in the responses of PCs located in the palm. In addition, preserving spatial structure is more beneficial for capturing gestures involving single rather than multiple digits. This work contributes to further understanding the sense of touch by introducing novel measurement-driven computational methods for analyzing the population-level neural representations of natural touch gestures over multiple spatiotemporal scales.**

***Index Terms*—Haptic neuroscience, Natural touch gestures, Tactile information encoding, Neural spiking classification.**

I. Introduction

Touch interactions performed with the hands elicit mechanical vibrations that propagate throughout the skin [1]–[5]. These propagating vibrations facilitate touch perception by exciting responses in widespread populations of sensory neurons [6]–[8], including those innervating Pacinian corpuscles (PCs). PCs have large receptive fields [9] and are exquisitely sensitive to vibrations elicited by touch interactions such as fine manipulation, texture scanning, and tool use [10]–[12]. While spiking responses of isolated PCs elicited by laboratory stimuli are thoroughly characterized [13]–[15], the responses of PC populations throughout the hand are not well understood. In addition, few studies have examined PC responses to propagating vibrations originating at locations far removed from the PC locations. This is partly due to experimental limitations that preclude the measurement of signals from PC populations in an unconstrained hand [16].

This work was supported by a Link Foundation Modeling, Simulation, and Training Fellowship to N.T., the German Research Foundation DFG Project EXC 2050/1, 390696704, for the TU Dresden CeTI Cluster of Excellence to Y.S., and U.S. National Science Foundation award 1751348 to Y.V.

Previous research has underscored the significance of investigating population encoding in understanding the sense of touch [17], [18]. Numerous studies have characterized the responses of tactile neuron populations to controlled laboratory stimuli, examining parameters such as intensity [19], [20], frequency [21], textural vibration content [22]–[24], and edge orientation [25], and demonstrated that touch information is encoded at various spatial and temporal scales. To explore the spatiotemporal structure of information encoded in population responses, several investigations, including those in other areas of sensory neuroscience, have utilized stimulus discrimination tasks conducted via metric space and classification methods [21], [25]–[31]. However, our understanding of information encoding within the spatiotemporal organization of PC population responses in natural contexts remains limited.

In this paper, we employ a novel measurement-driven approach for simulating the responses of a spatially-distributed population of PCs in the hand during natural touch interactions. Leveraging existing vibrometry measurements of whole-hand skin motion collected during commonly performed tapping, sliding, and grasping gestures involving contact at the digits [1], [2], we drive an ensemble of neuron models developed in prior research [32]. We then utilize several machine learning techniques to investigate the spatiotemporal encoding of information generated by these touch interactions in PC population responses. We find that preserving spatial structure in whole-hand PC responses is beneficial for capturing gesture-specific information, particularly for single-digit gestures, while retaining spike timing becomes more informative for gesture representation by PCs located in the palm. The findings and methodologies presented here may contribute to knowledge about the spatiotemporal organization of touch information in PC population responses and may inform the engineering of new haptic or robotic technologies that reflect attributes of tactile sensing and perception in the human hand [33]–[36].

In the following section, we describe our methods for integrating spiking neuron models [32] with mechanical measurements [1], [2], computing population spiking response representations by multi-scale spatiotemporal integration, and analyzing information content preserved by these representations using machine-learning techniques. We then discuss and analyze the results of these studies and their implications

979-8-3503-9993-6/23/$31.00 © 2023 IEEE

2023 IEEE World Haptics Conference (WHC)
WHC 2023, Delft, Netherlands, July 10–13, 2023

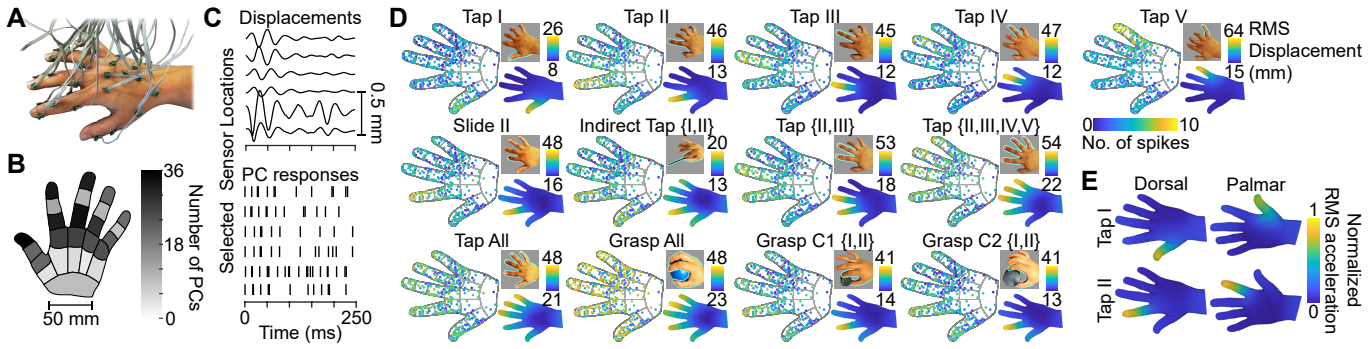

Fig. 1. A) Placement of the accelerometer array on the dorsal surface of a participant's hand [1], [2]. B) Number of PCs uniformly distributed within each region of the hand, derived from [37]. C) Skin displacements (top) and corresponding PC spiking responses (bottom) at selected sensor locations during one trial of the Slide II gesture. D) Shown for each of the 13 performed gestures: number of spikes produced by each PC in the hand averaged across all trials of the gesture (left), an image of a participant executing the gesture (top right), and RMS skin displacements elicited across the whole hand during the gesture (bottom right). E) RMS skin accelerations elicited across the dorsal (left column) and volar (right column) surfaces of the hand during one trial of the Tap I gesture (top row) and one trial of the Tap II gesture (bottom row), normalized by the maximum skin acceleration produced during each trial [2].

for touch information encoding in PC population responses. We conclude by synthesizing these findings and discussing their significance for haptic science and engineering and opportunities for future research.

II. Methods

Using the methods detailed in this section, we sought to quantify how much touch gesture information was retained in PC population responses at different spatial and temporal scales. PC population responses were generated by driving physiologically-informed neuron models adapted from previous research [32] with an existing vibrometry dataset of skin motion measurements collected during everyday touch interactions [1], [2]. To modify the spatiotemporal structure of these population responses, we summed spiking data over spatial and temporal bins of different sizes, allowing us to capture touch gesture information at multiple spatiotemporal scales. We then used machine learning classifiers to analyze how much gesture information was preserved in these spatiotemporal response representations.

A. Whole-Hand Skin Vibrometry Data

Our methodology leveraged an existing dataset of whole-hand skin vibration measurements captured in a prior experiment during manual touch gestures performed by four participants using an array of 30 miniature accelerometers [1], [2]. The accelerometers were worn on the dorsal surface of the hand during data collection, allowing unobstructed movement during gesture execution (Fig. 1A). Accelerometers were placed at the same relative anatomical positions on each hand, standardizing their locations across participants. The gestures were comprised of commonly performed manual interactions (Fig. 1D). Each gesture was repeated for either 100 (grasping gestures) or 200 (all other gestures) trials. The patterns of skin vibrations elicited during gestures involving fingertip movement were found to be similar between the volar and dorsal surfaces of the hand in a prior investigation (Fig. 1E) [2], allowing the utilization of the dorsal skin oscillation measurements as an approximation of volar skin motion.

Data from each trial were time-aligned with respect to the instant of surface or object contact, truncated to a duration of 250 ms, and band-pass filtered between 20-500 Hz. Acceleration measurements were converted to displacement via double integration. To facilitate analysis, the three-axis data from each sensor were independently projected to a principal axis of oscillation through principal component analysis (PCA). The projection maximally preserved variance in the data. The processed data from each trial consisted of time-varying signals of 250 ms duration sampled at 2.0 kHz from each of 30 accelerometers, yielding 15000 samples per trial. The dataset consisted of 4564 trials in total.

B. Vibrometry-Driven Neural Simulations

The processed skin displacement signals were used as inputs to a population of K physiologically-informed PC neuron models [32] that produced spiking responses for each trial, where $K = 490$ unless otherwise specified (Fig. 1C, D). The highly stereotyped and reproducible responses of PCs were captured with high fidelity by the utilized neuron models, which were trained and extensively validated on microneurography data collected from macaque monkeys in prior research [19]. PCs were distributed across a 3D hand model according to a recent MRI study on PC distribution in the glabrous skin that dictated the number of PCs that were uniformly distributed within each hand region (Fig. 1B) [37]. Skin displacements were interpolated to each PC location using an inverse distance filter informed by biomechanical measurements and described in a previous publication [2], with distance calculated on the dorsal surface of the 3D hand model.

C. Spatiotemporal Spike Count Representations

To analyze the PC population responses at various temporal scales, six time bin widths, Δt, were defined in decreasing order of preserved temporal resolution. These widths were $\Delta t \in \{5, 10, 25, 50, 125, 250\}$ ms, and the number of time bins was calculated as $N = \frac{250}{\Delta t} = \{50, 25, 10, 5, 2, 1\}$. To analyze the PC population responses at various spatial scales,

two distinct collections of sets of spatial bins were defined, with one collection encompassing the whole hand (WH) and the other encompassing only the palm (P). A set of spatial bins was defined as a set of M non-overlapping contiguous spatial regions in the hand based on anatomical regions defined in Fig. 2A. To analyze the whole-hand PC population responses, four sets of spatial bins, each denoted as $\mathbf{s}$, were defined in decreasing order of preserved spatial resolution, as illustrated in Fig. 2B. They were as follows:

1) $\mathbf{s}$ = WH1, $M = K$: Each PC in the hand ($K = 490$, unless otherwise specified),
2) $\mathbf{s}$ = WH2, $M = 25$: the distal phalanges (DP), medial phalanges (MP), proximal phalanges (PP), metacarpophalangeal joint regions (MCP), and metacarpal (MC) regions corresponding to each digit (I-V) and the carpal (C) region of the palm,
3) $\mathbf{s}$ = WH3, $M = 6$: each digit (I-V) and the palm,
4) $\mathbf{s}$ = WH4, $M = 1$: and the whole hand.

To analyze PC population responses from the palm, five sets of spatial bins, each denoted as $\mathbf{s}_p$, were defined in decreasing order of preserved spatial resolution, as illustrated in Fig. 2C. They were as follows:

1) $\mathbf{s}_p$ = P1, $M = 162$: Each PC in the palm,
2) $\mathbf{s}_p$ = P2, $M = 11$: the MCP and MC regions corresponding to each digit (I-V) and C,
3) $\mathbf{s}_p$ = P3, $M = 3$: the Palm {I,II}, Palm III, and Palm {IV,V} regions,
4) $\mathbf{s}_p$ = P4, $M = 3$: all MCP, MC, and C regions without digit separation,
5) $\mathbf{s}_p$ = P5, $M = 1$: and the whole palm.

Using these bins, the PC population spiking response for each trial was quantified as a binned spike train matrix B of size $M \times N$, where M was the number of spatial bins and N was the number of time bins. The element B_{ij} contained the number of spikes generated in time bin j by PCs situated in spatial bin i. This representation allowed us to control the spatiotemporal resolution of the population responses by manipulating the bin sizes without employing dimensionality reduction methods that would complicate the analysis.

The sets of spatial bins ranged from preserving individual neuron identity of spikes ($\mathbf{s}$ = WH1 or $\mathbf{s}_p$ = P1) to aggregating spikes across the whole PC population ($\mathbf{s}$ = WH4 or $\mathbf{s}_p$ = P5), as shown for one trial of the Grasp All gesture (Fig. 2D). Similarly, the time bin widths varied from capturing detailed spike timing ($\Delta t = 5\,\text{ms}$) to summing spike counts over the entire trial ($\Delta t = 250\,\text{ms}$), as demonstrated for one trial of the Tap V gesture (Fig. 2E). These variations in spatiotemporal representations impacted the degree to which differences in PC population responses evoked by various natural touch gestures were captured.

D. Evaluation of Touch Information in Spatiotemporal Spike Count Representations

We employed four non-parametric classification methods to elucidate the amount of information encoded in the spatiotemporal structure of PC population responses elicited by natural touch gestures. These methods included a linear kernel support vector machine (SVM), a k-nearest neighbors classifier (kNN), a peristimulus spike timing histogram (PSTH) template-based classifier (PTB) [26], [27], and an average pairwise distance classifier (APD). These techniques were applied to binned spike train matrices to analyze the extent to which PC population responses retained information across spatiotemporal scales.

For the SVM and kNN classifiers, reported classification accuracies were averaged over a 10-fold cross-validation procedure with a random 90-10 train-test split. For the SVM classifier, each feature was standardized using the mean and standard deviation calculated from the training dataset. For kNN, $k = 5$ was chosen based on parameter selection during pre-testing. The kNN and APD classifiers utilized a distance matrix composed of pairwise Euclidean distances between

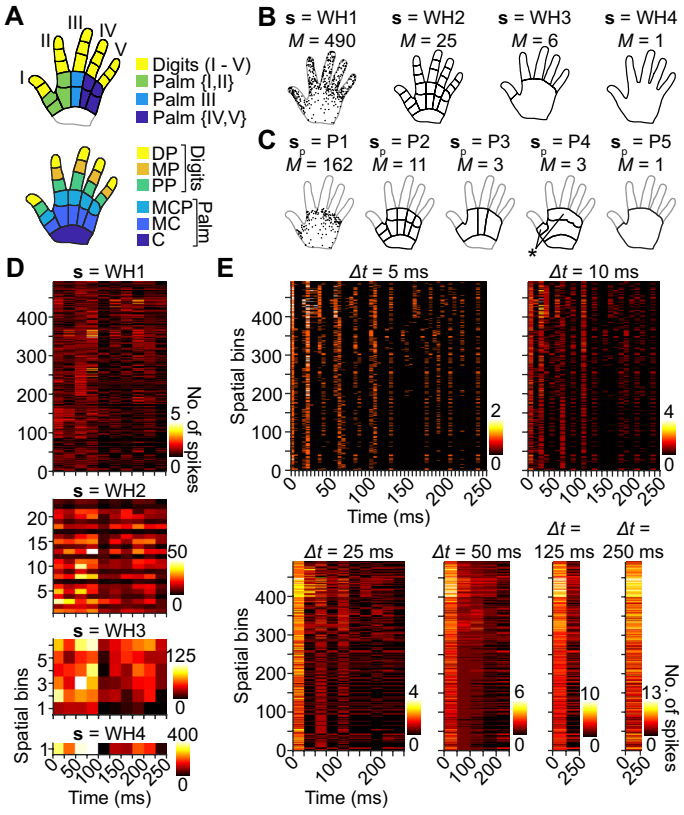

Fig. 2. A) Anatomically-based hand regions defined for spatial resolution analyses. Within the digits, DP are distal phalanges, MP are medial phalanges, and PP are proximal phalanges. Within the palm, MCP are metacarpophalangeal joint regions, MC are metacarpal regions, and C is the carpal region. B) Four sets of spatial bins ($\mathbf{s}$ = WH1-WH4) defined for whole-hand analyses where M is the size of each set. Each PC in the hand is considered a separate spatial bin in WH1. Each spatial bin in WH2-WH4 is outlined by solid black lines. C) Five sets of spatial bins ($\mathbf{s}_p$ = P1-P5) defined for analyses in the palm where M is the size of each set. Each PC in the palm is considered a separate spatial bin in P1. Each spatial bin in P2-P5 is outlined by solid black lines. Regions outlined by light gray lines are not included in the spatial bins. Regions indicated by the star label (*) in P4 are part of the same spatial bin. D) Binned spike train matrices representing a PC population response elicited by one trial of the Grasp All gesture shown across all sets of whole-hand spatial bins $\mathbf{s}$ = WH1-WH4 when $\Delta t = 25\,\text{ms}$. E) Binned spike train matrices representing a PC population response elicited by one trial of the Tap V gesture shown across all time bin widths Δt when $\mathbf{s}$ = WH1.

binned spike train matrices for all trials. For the PTB and APD classifiers, results were averaged over a leave-one-out cross-validation procedure where each trial was successively designated as the test set while the rest of the dataset comprised the training set. For the PTB classifier, template PSTHs were calculated for each gesture by taking the element-wise average over binned spike train matrices from all trials of the gesture, excluding the test trial. The test trial was then classified as the gesture corresponding to the PSTH for which the pairwise Euclidean distance was the smallest. The APD classifier classified each test trial as the gesture corresponding to the training samples for which the average pairwise Euclidean distance to the test trial was the smallest.

III. Results: Spatiotemporal Organization of Touch Information in PC Population Responses

The responses of tactile neuron populations encode information about mechanical stimuli in both the spike timing and the identity of neurons generating each spike [21], [22], [24], [25]. Here, we presented the results of our investigation on how information about natural touch gestures was preserved in spike count representations at multiple spatiotemporal scales and within hand regions away from the contact location. We quantified the captured information through the overall and per-gesture classification accuracies achieved by several non-parametric classification methods.

A. Varying the Spatiotemporal Resolution of Spike Count Representations

1) Whole-Hand PC Population Responses: Our analysis showed that modifying the spatial resolution of spike count representations had a greater impact on touch gesture classification than modifying the temporal resolution. When individual neuron identity was preserved and temporal structure eliminated ($\mathbf{s}$ = WH1, $\Delta t = 250\,\text{ms}$), the average classification accuracy was 75 % for SVM, 73 % for kNN, and 46 % for PTB and APD (Fig. 3A). On the other hand, when precise spike timing was preserved and spatial structure eliminated ($\mathbf{s}$ = WH4, $\Delta t = 5\,\text{ms}$), the average classification accuracy dropped significantly: by 33 % for SVM, 28 % for kNN, 15 % for PTB, and 18 % for APD. Additionally, the median range of classification accuracies across changes in spatial resolution was greater than that across changes in temporal resolution by a factor of at least 2 for all classifiers (Fig. 3B). When some spatial structure was preserved ($\mathbf{s}$ = WH1, WH2, or WH3), all classifiers performed best at $\Delta t = 25$-$50\,\text{ms}$, suggesting that an intermediate level of temporal integration was beneficial in accommodating variations in touch information across trials.

While the goal of this research was not to analyze the suitability of classification methods for this gesture discrimination task, the findings showed that SVM performed best for all spatiotemporal representations except when $\mathbf{s}$ = WH4, where it was outperformed by kNN for $\Delta t \leq 25\,\text{ms}$. On the other hand, PTB and APD achieved the lowest average classification accuracies except at coarse spatiotemporal resolution ($\Delta t \geq 125\,\text{ms}$ and $\mathbf{s}$ = WH4), demonstrating that they were more sensitive

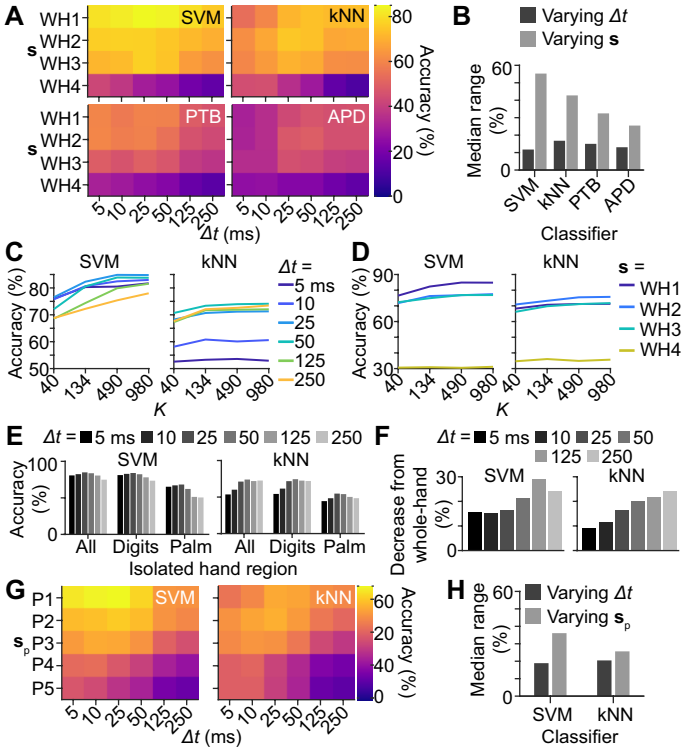

Fig. 3. A) Matrix of average classification accuracies achieved using whole-hand PC responses for all combinations of Δt and $\mathbf{s}$ by all classifiers. B) Median range of classification accuracies using whole-hand PC responses across changes in Δt (dark gray) and across changes in $\mathbf{s}$ (light gray) for all classifiers. C) Classification accuracy as the total number of PCs in the hand K varies for all Δt when $\mathbf{s}$ = WH1. D) Classification accuracy as the total number of PCs in the hand K varies for all $\mathbf{s}$ when $\Delta t = 25\,\text{ms}$. C) and D) are shown for both SVM (left) and kNN (right). E) Average classification accuracies using PC responses from the whole hand (All), from only the digits (Digits), and from only the palm (Palm) for all Δt. Shown for SVM (left) and kNN (right). F) Decrease in average classification accuracy from using whole-hand PC responses to using PC responses from the palm for all Δt. Shown for SVM (left) and kNN (right). There was no spatial integration performed for E) and F); each PC was a separate spatial bin. G) Matrix of average classification accuracies achieved using PC responses from the palm for all combinations of Δt and $\mathbf{s}_p$ by SVM (left) and kNN (right). H) Median range of classification accuracies using PC responses from the palm across changes in Δt (dark gray) and across changes in $\mathbf{s}_p$ (light gray) for SVM (left) and kNN (right).

than other methods to small perturbations between trials. The remaining analyses focus on SVM and kNN, as they performed better than PTB and APD in almost all cases and are sufficient to represent our overall findings, which are consistent across all classifiers. Additionally, as the results were robust to scaling of the PC population size (Fig. 3C, D), $K = 490$ was utilized for all other analyses.

2) PC Population Responses From the Palm: Analyses of responses from PCs restricted to the digits yielded gesture classification accuracies nearly as high as those obtained from whole-hand PC responses at all temporal resolutions (Fig. 3E), likely due in part to the large proportion of touch contacts that occurred at the digits in the utilized dataset. However, prior findings have demonstrated that tactile neurons remote from the stimulus location can encode touch information via mechanical

wave propagation [6], [7], [21]. This motivated our subsequent analysis of gesture encoding at various spatiotemporal scales by PC subpopulations restricted to the palm.

Consistent with the findings from the aforementioned studies, our results showed that gestures were readily recognized when PCs were isolated in the palm. Average classification accuracy was 66 % in the best case (SVM, $\mathbf{s}_p$ = P1, Δt = 25 ms) (Fig. 3E, G). The smallest decrease in performance from whole-hand classification occurred at fine temporal resolutions ($\Delta t \leq$ 10 ms) (Fig. 3F). This finding demonstrates that without the contribution of spiking responses from PCs located in the digits, precise spike timing played a larger role in gesture discrimination.

Similar to whole-hand analysis results (Fig. 3B), classification accuracy varied more across changes in spatial resolution than temporal resolution (Fig. 3H). However, the median range of classification accuracies increased by 5 % for changes in temporal resolution while decreasing by nearly 20 % for changes in spatial resolution compared to the whole-hand analysis results for both classifiers. This finding again indicates that the preservation of temporal structure became more consequential for the representation of touch gestures by PC subpopulations in the palm.

Nonetheless, spatial structure still impacted the encoding of gesture information in the palm. Classification accuracy was significantly higher when PC responses were integrated across palmar regions oriented along the axis of the digits ($\mathbf{s}_p$ = P3) than when integrated across regions oriented orthogonal to the digits ($\mathbf{s}_p$ = P4), despite both sets containing an equal number of spatial regions ($M = 3$) (Fig. 3G). The integration of spikes over $\mathbf{s}_p$ = P3 effectively preserved information about individual digits or pairs of digits, while such preservation was absent in the integration of spikes over $\mathbf{s}_p$ = P4. These results demonstrate the importance of retaining a minimal level of digit separation within the spatial structure of the spike count representations.

B. Varying the Spatiotemporal Resolution of Gesture-Level Spike Count Representations

We next explored the representation of touch information associated with individual gestures across variations in the spatiotemporal resolution of whole-hand spike count representations. Single-digit gestures were better represented than multi-digit gestures under most spatiotemporal conditions, except when spatial information was eliminated ($\mathbf{s}$ = WH4) (Fig. 4A, B). In addition, single-digit gestures were classified most accurately when Δt = 10-25 ms, while multi-digit gestures were best captured at a lower temporal resolution (Δt = 50 ms). These performance differences between gesture types may have been a consequence of high trial-to-trial variability in the timing of contact with the target surface or object by the individual digits involved in the multi-digit gestures.

Additionally, we found that spatial structure played a larger role in representing single-digit gestures, while temporal structure was more consequential for capturing multi-digit gestures. The median range of classification accuracies when

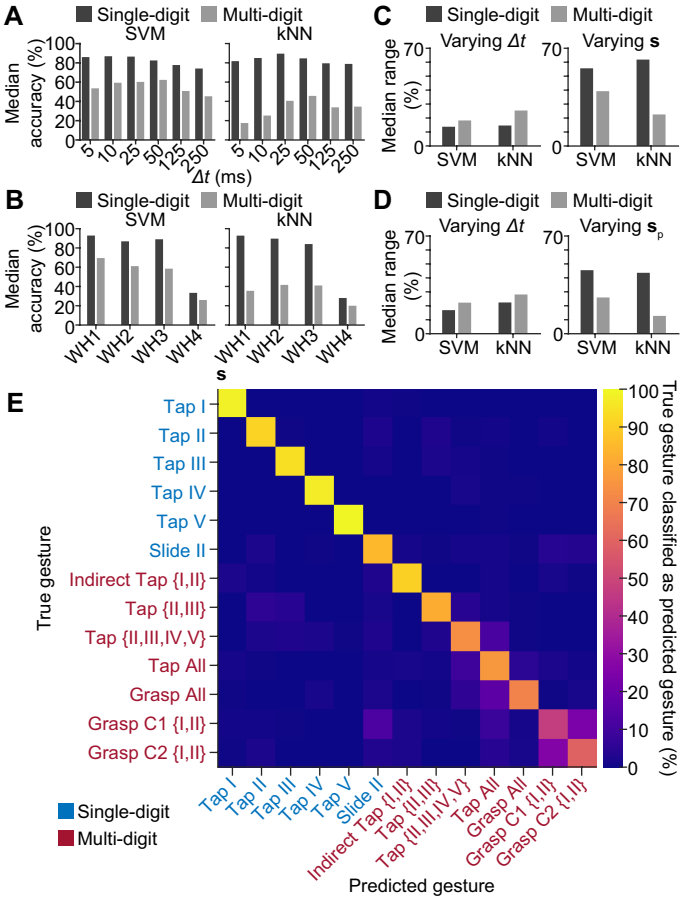

Fig. 4. A) Median classification accuracy of single-digit (dark gray) and multi-digit (light gray) gestures for all Δt using whole-hand PC responses. The median is computed across all $\mathbf{s}$ and all single- or multi-digit gestures. B) Median classification accuracy of single-digit (dark gray) and multi-digit (light gray) gestures for all $\mathbf{s}$ using whole-hand PC responses. The median is computed across all Δt and all single- or multi-digit gestures. C) Median range of classification accuracies of single-digit (dark gray) and multi-digit (light gray) gestures across changes in Δt (left) and across changes in $\mathbf{s}$ (right) using whole-hand PC responses. D) Median range of classification accuracies of single-digit (dark gray) and multi-digit (light gray) gestures across changes in Δt (left) and across changes in $\mathbf{s}_p$ (right) using PC responses from the palm. In C) and D), when varying Δt, the median is computed over all $\mathbf{s}$ or $\mathbf{s}_p$ and all single- or multi-digit gestures. Similarly, when varying $\mathbf{s}$ or $\mathbf{s}_p$, the median is computed over all Δt and all single- or multi-digit gestures. E) Confusion matrix showing the percent of each gesture (True) classified as another gesture (Predicted) for the best-performing classifier (SVM, $\mathbf{s}$ = WH1, Δt = 25 ms) using whole-hand PC responses. Per-gesture classification accuracy is read from the diagonal of the matrix. False positives are read from the columns, and false negatives are read from the rows.

varying spatial resolution was greater for single-digit gestures, while the median range when varying temporal resolution was slightly greater for multi-digit gestures (Fig. 4C). This trend was preserved for PC responses from the palm (Fig. 4D). Though spatial structure still played a significant role in encoding multi-digit gestures, it was more beneficial for representing single-digit gestures.

For the best-performing classifier (SVM, Δt = 25 ms, $\mathbf{s}$ = WH1), most misclassifications occurred between cylinder grasps (Grasp C1 {I,II} and Grasp C2 {I,II}) and between

gestures requiring most or all of the digits (Tap {II,III,IV,V}, Tap All, and Grasp Ball All) (Fig. 4E). Cylinder grasps were commonly confused because they were identical apart from the cylinder sizes, varying in radius by only $1.6\,\mathrm{cm}$. Misclassifications also occurred between single-digit tapping gestures and between Slide II and cylinder grasps. PC population responses in the palm contained less information enabling the distinction between multi-digit gestures and their component single-digit gestures. This was demonstrated by misclassifications between Tap {II,III} and its corresponding single-digit gestures Tap II and Tap III and between the cylinder grasps and their constituent single-digit gestures Tap I and Tap II. Further misclassifications occurred between multi-digit taps and grasps.

IV. Discussion and Conclusion

Our work investigated the spatiotemporal organization of touch information in PC population spiking responses elicited during common touch gestures. We examined the amount of gesture information preserved within the responses at different spatiotemporal scales via a novel vibrometry-driven neural simulation method adapted from prior research [1], [2], [32]. The elicited PC population responses were spatiotemporally integrated and analyzed using several machine learning techniques. Our results showed that the spatial structure of PC population responses played a significant role in encoding information about touch gestures, especially single-digit gestures. The temporal structure of PC population responses was also meaningful, particularly for PCs in the palm.

While these findings necessarily reflect the scope of the included gestures, which do not capture the full range of manual interactions involved in all activities, they nevertheless furnish insight into the spatiotemporal organization of natural touch information in PC population responses in conditions with greater ecological validity than are generally probed in many laboratory experiments. The analyzed dataset included several multi-finger tapping and grasping gestures and many gestures engaging one or two digits. The selection of gestures was informed by prior studies demonstrating that the majority of natural contact events occur at the fingertips [38]. Our findings suggest that the relative importance of temporal structure in touch information encoding within PC population responses may have been enhanced if the analyzed dataset placed greater emphasis on grasping or multi-digit gestures.

Although the methods employed here are approximate, few alternatives are available since existing methods preclude the measurement of neural population responses in the periphery during natural touch behavior. Multiple classification methods and parameters were employed to validate the findings presented here. Despite variations between results obtained with different classifiers, which may reflect differences in their expressive capacity, qualitatively similar findings were obtained from different classification techniques. In addition, results were consistent across changes in PC population size for all spatiotemporal parameters. Moreover, the spatiotemporal spike count representations employed for classification analysis condensed the raw spiking data without the need for intermediary assumptions or dimensionality reduction techniques.

The findings of our study are generally consistent with prior research on the neural processing of tactile inputs and attributes of somatosensory representations in the periphery and brain. Highlighting the role of spatial structure in tactile encoding, studies have shown that representations of different digits in the primary somatosensory cortex (S1) have distinct spatial properties, with larger areas dedicated to the digits that are most sensitive and agile, such as the thumb and index finger [39]. Recent work has also indicated that biomechanical coupling in the hand facilitates a hierarchical organization of tactile information in a gradient from fine (individuated digits) to coarse (whole-hand) spatial representations [2]. Though the correspondence of those findings to representations in the brain remains unclear, they point to the utility of spatial structure in peripheral tactile processing. Our results further underscore the importance of digit-specific spatial structure in peripheral neural representations of tactile interactions.

Prior research has also shown that tactile neurons in the periphery and S1 exhibit a high degree of temporal precision, demonstrating the role of temporal structure in the encoding of touch events [21], [40]. Additionally, our results reflected dependence on the gesture or action being represented, aligning with prior research showing that the involvement of spatial and temporal information in somatosensory processing is task and stimulus-dependent [22], [24], [25]. Furthermore, prior studies have demonstrated that tactile neurons terminating at locations far from the location of skin-object contact can encode information about haptic properties, such as surface roughness, due to biomechanical coupling in the skin [4], [6], [7]. Those observations support our findings that substantial information is contained in responses of PC populations in palmar areas and highlight the potential significance of biomechanical coupling in tactile information encoding.

It is important to note that several of the aforementioned studies reflect the processing of peripheral spiking inputs from multiple mechanoreceptive pathways within the dorsal column and effects of cortical processing in S1 [41]–[43], which were not accounted for in our study. Further analysis is needed to relate our findings to research on the spatiotemporal organization of touch information in early and cortical processing. Nonetheless, our results underline the significance of spatial and temporal organization at multiple scales for the peripheral neural processing of tactile information.

The methodology applied here illustrates how mechanisms of tactile information processing can be investigated through the combination of mechanical measurements and neural simulations. Our findings may inform the development of novel computational models of tactile information encoding by populations of sensory neurons and contribute to the engineering of technologies for haptic feedback or robotic touch sensing [33]–[36]. Future studies may incorporate other mechanoreceptive neuron types (SA1 and RA), larger datasets of natural touch interactions, or analysis techniques drawn from other areas of sensory neuroscience [44], [45].

REFERENCES

[1] Yitian Shao, Vincent Hayward, and Yon Visell. Spatial patterns of cutaneous vibration during whole-hand haptic interactions. *Proceedings of the National Academy of Sciences*, 113(15):4188–4193, 2016.

[2] Yitian Shao, Vincent Hayward, and Yon Visell. Compression of dynamic tactile information in the human hand. *Science Advances*, 6(16):eaaz1158, 2020.

[3] Bharat Dandu, Yitian Shao, and Yon Visell. Rendering spatiotemporal haptic effects via the physics of waves in the skin. *IEEE Transactions on Haptics*, 14(2):347–358, 2021.

[4] Louise R. Manfredi, Andrew T. Baker, Damian O. Elias, John F. Dammann Iii, Mark C. Zielinski, Vicky S. Polashock, and Sliman J. Bensmaia. The effect of surface wave propagation on neural responses to vibration in primate glabrous skin. *PLOS ONE*, 7(2):e31203, 2012.

[5] Louise R. Manfredi, Hannes P. Saal, Kyler J. Brown, Mark C. Zielinski, John F. Dammann, Vicky S. Polashock, and Sliman J. Bensmaia. Natural scenes in tactile texture. *Journal of Neurophysiology*, 111(9):1792–1802, 2014.

[6] Benoit Delhaye, Vincent Hayward, Philippe Lefèvre, and Jean-Louis Thonnard. Texture-induced vibrations in the forearm during tactile exploration. *Frontiers in Behavioral Neuroscience*, 6, 2012.

[7] Xavier Libouton, Olivier Barbier, Yorick Berger, Leon Plaghki, and Jean-Louis Thonnard. Tactile roughness discrimination of the finger pad relies primarily on vibration sensitive afferents not necessarily located in the hand. *Behavioural Brain Research*, 229(1):273–279, 2012.

[8] J. W. Andrews, M. J. Adams, and T. D. Montenegro-Johnson. A universal scaling law of mammalian touch. *Science Advances*, 6(41):eabb6912, 2020.

[9] Roland S. Johansson and Åke B. Vallbo. Tactile sensory coding in the glabrous skin of the human hand. *Trends in Neurosciences*, 6:27–32, 1983.

[10] C. C. Hunt. On the nature of vibration receptors in the hind limb of the cat. *The Journal of Physiology*, 155(1):175–186, 1961.

[11] Sliman Bensmaïa and Mark Hollins. Pacinian representations of fine surface texture. *Perception & Psychophysics*, 67(5):842–854, 2005.

[12] Luke E. Miller, Luca Montroni, Eric Koun, Romeo Salemme, Vincent Hayward, and Alessandro Farnè. Sensing with tools extends somatosensory processing beyond the body. *Nature*, 561(7722):239–242, 2018.

[13] Jonathan Bell, Stanley Bolanowski, and Mark H. Holmes. The structure and function of pacinian corpuscles: A review. *Progress in Neurobiology*, 42(1):79–128, 1994.

[14] S. J. Bolanowski and J. J. Zwislocki. Intensity and frequency characteristics of pacinian corpuscles. i. action potentials. *Journal of Neurophysiology*, 51(4):793–811, 1984.

[15] M. Sato. Response of pacinian corpuscles to sinusoidal vibration. *The Journal of Physiology*, 159(3):391–409, 1961.

[16] Å B. Vallbo and K.-E. Hagbarth. Activity from skin mechanoreceptors recorded percutaneously in awake human subjects. *Experimental Neurology*, 21(3):270–289, 1968.

[17] K O Johnson. Reconstruction of population response to a vibratory stimulus in quickly adapting mechanoreceptive afferent fiber population innervating glabrous skin of the monkey. *Journal of Neurophysiology*, 37(1):48–72, 1974.

[18] Hannes P. Saal and Sliman J. Bensmaia. Touch is a team effort: interplay of submodalities in cutaneous sensibility. *CellPress*, 2014.

[19] Michael A. Muniak, Supratim Ray, Steven S. Hsiao, J. Frank Dammann, and Sliman J. Bensmaia. The neural coding of stimulus intensity: Linking the population response of mechanoreceptive afferents with psychophysical behavior. *Journal of Neuroscience*, 27(43):11687–11699, 2007.

[20] Sliman J. Bensmaia. Tactile intensity and population codes. *Behavioural Brain Research*, 190(2):165–173, 2008.

[21] Emily L. Mackevicius, Matthew D. Best, Hannes P. Saal, and Sliman J. Bensmaia. Millisecond precision spike timing shapes tactile perception. *The Journal of Neuroscience*, 32(44):15309, 2012.

[22] Alison I Weber, Hannes P Saal, Justin D Lieber, Ju-Wen Cheng, Louise R Manfredi, John F Dammann III, and Sliman J Bensmaia. Spatial and temporal codes mediate the tactile perception of natural textures. *Proceedings of the National Academy of Sciences*, 110(42):17107–17112, 2013.

[23] Katie H Long, Justin D Lieber, and Sliman J Bensmaia. Texture is encoded in precise temporal spiking patterns in primate somatosensory cortex. *Nature Communications*, 13(1):1311, 2022.

[24] Michael A. Harvey, Hannes P. Saal, John F. Dammann Iii, and Sliman J. Bensmaia. Multiplexing stimulus information through rate and temporal codes in primate somatosensory cortex. *PLOS Biology*, 11(5):e1001558, 2013.

[25] Etay Hay and J. Andrew Pruszynski. Orientation processing by synaptic integration across first-order tactile neurons. *PLOS Computational Biology*, 16(12):e1008303, 2020.

[26] Guglielmo Foffani and Karen Anne Moxon. Psth-based classification of sensory stimuli using ensembles of single neurons. *Journal of Neuroscience Methods*, 135(1):107–120, 2004.

[27] Guglielmo Foffani, John K. Chapin, and Karen A. Moxon. Computational role of large receptive fields in the primary somatosensory cortex. *Journal of Neurophysiology*, 100(1):268–280, 2008.

[28] Dmitriy Aronov, Daniel S. Reich, Ferenc Mechler, and Jonathan D. Victor. Neural coding of spatial phase in v1 of the macaque monkey. *Journal of Neurophysiology*, 89(6):3304–3327, 2003.

[29] Austin J. Brockmeier, John S. Choi, Evan G. Kriminger, Joseph T. Francis, and Jose C. Principe. Neural decoding with kernel-based metric learning. *Neural Computation*, 26(6):1080–1107, 2014.

[30] Zihan Pan, Jibin Wu, Malu Zhang, Haizhou Li, and Yansong Chua. Neural population coding for effective temporal classification. In *2019 International Joint Conference on Neural Networks (IJCNN)*, page 1–8, 2019.

[31] Eero Satuvuori, Mario Mulansky, Andreas Daffertshofer, and Thomas Kreuz. Using spike train distances to identify the most discriminative neuronal subpopulation. *Journal of Neuroscience Methods*, 308:354–365, 2018.

[32] Hannes P. Saal, Benoit P. Delhaye, Brandon C. Rayhaun, and Sliman J. Bensmaia. Simulating tactile signals from the whole hand with millisecond precision. *Proceedings of the National Academy of Sciences*, 114(28):E5693–E5702, 2017.

[33] Rochelle Ackerley and Anne Kavounoudias. The role of tactile afference in shaping motor behaviour and implications for prosthetic innovation. *Neuropsychologia*, 79:192–205, 2015.

[34] Sung Soo Kim, Arun P. Sripati, R. Jacob Vogelstein, Robert S. Armiger, Alexander F. Russell, and Sliman J. Bensmaia. Conveying tactile feedback in sensorized hand neuroprostheses using a biofidelic model of mechanotransduction. *IEEE Transactions on Biomedical Circuits and Systems*, 3(6):398–404, 2009.

[35] Sliman J. Bensmaia. Biological and bionic hands: natural neural coding and artificial perception. *Philosophical Transactions of the Royal Society B: Biological Sciences*, 370(1677):20140209, 2015.

[36] J Dargahi and S Najarian. Human tactile perception as a standard for artificial tactile sensing—a review. *The International Journal of Medical Robotics and Computer Assisted Surgery*, 1(1):23–35, 2004.

[37] Christoph Germann, Reto Sutter, and Daniel Nanz. Novel observations of pacinian corpuscle distribution in the hands and feet based on high-resolution 7-t mri in healthy volunteers. *Skeletal Radiology*, 50(6):1249–1255, 2021.

[38] Franck Gonzalez, Florian Gosselin, and Wael Bachta. Analysis of hand contact areas and interaction capabilities during manipulation and exploration. *IEEE Transactions on Haptics*, 7(4):415–429, 2014.

[39] Mriganka Sur. Receptive fields of neurons in areas 3b and 1 of somatosensory cortex in monkeys. *Brain research*, 198(2):465–471, 1980.

[40] Roland S Johansson and Ingvars Birznieks. First spikes in ensembles of human tactile afferents code complex spatial fingertip events. *Nature neuroscience*, 7(2):170–177, 2004.

[41] Fredrik Bengtsson, Romain Brasselet, Roland S Johansson, Angelo Arleo, and Henrik Jörntell. Integration of sensory quanta in cuneate nucleus neurons in vivo. *PloS one*, 8(2):e56630, 2013.

[42] Esther P Gardner and Richard M Costanzo. Spatial integration of multiple-point stimuli in primary somatosensory cortical receptive fields of alert monkeys. *Journal of Neurophysiology*, 43(2):420–443, 1980.

[43] Esther P Gardner and Richard M Costanzo. Temporal integration of multiple-point stimuli in primary somatosensory cortical receptive fields of alert monkeys. *Journal of Neurophysiology*, 43(2):444–468, 1980.

[44] Hannes Saal, Xiaoqin Wang, and Sliman Bensmaia. Importance of spike timing in touch: an analogy with hearing? *Current Opinion in Neurobiology*, 40:142–149, 2016.

[45] G. v. Békésy. Human skin perception of traveling waves similar to those on the cochlea. *The Journal of the Acoustical Society of America*, 27(5):830–841, 1955.